Article:
Dall'Ara, E., Bodey, A.J., Isaksson, H. et al. (2022) A practical guide for in situ mechanical testing of musculoskeletal tissues using synchrotron tomography. Journal of the Mechanical Behavior of Biomedical Materials, 133. 105297. ISSN: 1751-6161

https://doi.org/10.1016/j.jmbbm.2022.105297

journal of the mechanical behavior of biomedical materials 133 (2022) 105297

Contents lists available at ScienceDirect

Journal of the Mechanical Behavior of Biomedical Materials

journal homepage: www.elsevier.com/locate/jmbbm

A practical guide for *in situ* mechanical testing of musculoskeletal tissues using synchrotron tomography

E. Dall'Ara [a,b,*], A.J. Bodey [c], H. Isaksson [d,1], G. Tozzi [e,1]

[a] Department of Oncology and Metabolism, Mellanby Centre for Bone Research, University of Sheffield, UK
[b] INSIGNEO Institute for in Silico Medicine, University of Sheffield, UK
[c] Diamond Light Source, UK
[d] Department of Biomedical Engineering, Lund University, Lund, Sweden
[e] School of Engineering, London South Bank University, London, UK

ARTICLE INFO

Keywords:
X-ray tomography
Musculoskeletal
Biomaterials
Digital volume correlation
In situ mechanics

ABSTRACT

Musculoskeletal tissues are complex hierarchical materials where mechanical response is linked to structural and material properties at different dimensional levels. Therefore, high-resolution three-dimensional tomography is very useful for assessing tissue properties at different scales. In particular, Synchrotron Radiation micro-Computed Tomography (SR-microCT) has been used in several applications to analyze the structure of bone and biomaterials. In the past decade the development of digital volume correlation (DVC) algorithms applied to SR-microCT images and its combination with *in situ* mechanical testing (four-dimensional imaging) have allowed researchers to visualise, for the first time, the deformation of musculoskeletal tissues and their interaction with biomaterials under different loading scenarios. However, there are several experimental challenges that make these measurements difficult and at high risk of failure. Challenges relate to sample preparation, imaging parameters, loading setup, accumulated tissue damage for multiple tomographic acquisitions, reconstruction methods and data processing. Considering that access to SR-microCT facilities is usually associated with bidding processes and long waiting times, the failure of these experiments could notably slow down the advancement of this research area and reduce its impact. Many of the experimental failures can be avoided with increased experience in performing the tests and better guidelines for preparation and execution of these complex experiments; publication of negative results could help interested researchers to avoid recurring mistakes. Therefore, the goal of this article is to highlight the potential and pitfalls in the design and execution of *in situ* SR-microCT experiments, involving multiple scans, of musculoskeletal tissues for the assessment of their structural and/or mechanical properties. The advice and guidelines that follow should improve the success rate of this type of experiment, allowing the community to reach higher impact more efficiently.

1. Introduction

Musculoskeletal tissues are complex hierarchical materials where mechanical deformation is driven by structural and material properties at different dimensional levels. During the last 20 years, the study of their geometrical and morphological properties with high-resolution three-dimensional Synchrotron Radiation micro Computed Tomography (SR-microCT) has grown considerably (Salome et al., 1999; Peyrin et al., 2001; Obata et al., 2020). This technique enables the characterization of tissue microstructure in a minimally-invasive way and the resolution of features that would not be possible with standard desktop microCT systems. Both absorption and phase-contrast modalities can be used to evaluate the properties of hard and soft tissues, respectively. SR-microCT imaging has been used to evaluate the multiscale porosities of bone (Langer and Peyrin, 2016; Yu et al., 2020), the effects of ageing (Zimmermann et al., 2011) and anabolic treatments (Ma et al., 2017) on bone-tissue damage, the detailed microstructure and fiber arrangements in intervertebral discs (Disney et al., 2017), the microstructure of tendons (Zhou et al., 2018; Pierantoni et al., 2021), ligaments (Bergomi et al., 2010; Shearer et al., 2014), and cartilage (Coan et al., 2010; Nagarajan et al., 2014; Honkanen et al., 2020; Madi et al., 2020; Horng et al., 2021), the interface between cartilage and bone in the growth

* Corresponding author. Department of Oncology and Metabolism, Mellanby Centre for Bone Research, University of Sheffield, UK.
E-mail address: e.dallara@sheffield.ac.uk (E. Dall'Ara).
[1] authors share senior authorship.

https://doi.org/10.1016/j.jmbbm.2022.105297
Received 12 March 2022; Received in revised form 3 May 2022; Accepted 25 May 2022
Available online 31 May 2022

plate (Pierantoni et al., 2021), and the properties of biomaterials alone (Ehrenfried et al., 2010) or their integration with bone (Weiss et al., 2003; Fu et al., 2011; Mastrogiacomo et al., 2019).

Since its introduction (Bay, 1995; Nazarian et al., 2005), time-lapsed imaging of specimens under loading (also referred to as *in situ* testing) and digital volume correlation (DVC) have improved and enabled the study of how the geometrical, morphological and densitometric properties of biological tissues and biomaterials are related to their mechanical properties and their failure mechanisms. *In situ* testing within desktop microCT systems has been applied to a number of porous biological and engineering materials. Moreover, the DVC can be used to analyze local deformation induced by an applied load. In particular, the 3D images from *in situ* testing of the specimen in its undeformed and deformed configuration are fed to the DVC algorithms, which apply a deformable registration or cross-correlation function in order to compute the displacement (deflection) maps, which are subsequently differentiated into strain fields (Fig. 1) (Zauel et al., 2006; Chen et al., 2017). The results can then be shown in 4D images (values of displacement or strain as a function of space and loading step).

Initially based on input images acquired with desktop microCT, this approach has been used to characterize the mechanical properties of bone, which exhibits a number of natural features such as trabeculae and/or osteonal channels and other porosities, at different dimensional levels (Roberts et al., 2014; Grassi and Isaksson, 2015). The accuracy of DVC approaches can be evaluated from virtually deformed images (Christen et al., 2012), images from repeated scans to simulate zero-strain or constant-strain scenarios (Liu and Morgan, 2007), and virtually deformed images from repeated scans (Comini et al., 2019), with the last two approaches being preferable over the first as they account for the effect of image noise on the accuracy and precision of the method. The performance of different local or global DVC approaches in assessing 3D displacement and strain fields has been compared for the same bone specimens with and without biomaterials, highlighting their benefits and limitations (Dall'Ara, Peña-Fernández et al., 2016). The precision and accuracy will vary depending on many factors and should be investigated. As example, the precision of a global DVC approach (BoneDVC (Dall'Ara, Barber et al., 2014)), that depends on the considered structure, the image resolution and the DVC parameters, ranged from 0.02 μm for displacement measurements and 9 microstrains for average strain measurements (SR-microCT images, 1.6 μm voxel size, 300 μm spatial resolution, bovine cortical bone) to 7.29 μm for displacement measurements and 1547 microstrains for average strain measurements (in vivo microCT images, 10.4 μm voxel size, 300 μm spatial resolution, mouse tibia). The desktop microCT-based DVC approach has been used also in several applications for analyzing the mechanical behaviour of musculoskeletal tissues, for analyses on dentin (Lu et al., 2019), bone-biomaterial interfaces and residual damage after implant removal (Tozzi et al., 2014; Danesi et al., 2016; Joffre et al., 2017; Rapagna et al., 2019), trabecular bone (Zwahlen et al., 2015), whole vertebral bodies (Hosseini et al., 2014; Hussein et al., 2018), osteoarthritic femoral heads (Ryan et al., 2020), proximal femurs (Ridzwan et al., 2018), and implanted scapulae (Boulanaache et al., 2020). Furthermore, this approach has enabled the validation of local displacement and strain predicted by structural computational models such as the finite element method (Zauel et al., 2006; Chen et al., 2017; Jackman et al., 2016; Costa et al., 2017; Oliviero et al., 2018; Knowles et al., 2019), which were previously validated only for predictions of structural properties such as stiffness and strength (Dall'Ara, Luisier et al., 2013), qualitative comparison of failure distribution (Hosseini et al., 2014), or to back-calculate the local bone elastic modulus (Zwahlen et al., 2015). Strains in native soft tissues have been rarely evaluated with desktop microCT, due to the low absorption and thereby contrast in the images. Contrast agents have been used to enhance contrast in the soft tissues scanned with desktop microCT to study the full field deformation in osteochondral plugs (Clark et al., 2020) and human articular cartilage (Clark et al., 2021). However, it is still unknown how the staining approach affects the mechanical properties of the tissue. To the authors' knowledge, only one study tested the feasibility of DVC measurements on native cartilage using propagation-based phase contrast desktop microCT images (Tozzi et al., 2020). Sparse applications on ligaments (Naghibi et al., 2019) and intervertebral discs (Tavana et al., 2020; Tavana et al., 2020) have been performed from three-dimensional magnetic resonance imaging, but with limited resolution. In dental applications, high-resolution desktop microCT imaging in combination with *in situ* mechanical testing (Naveh et al., 2013) and Digital Image Correlation, applied on 2D images from the 3D

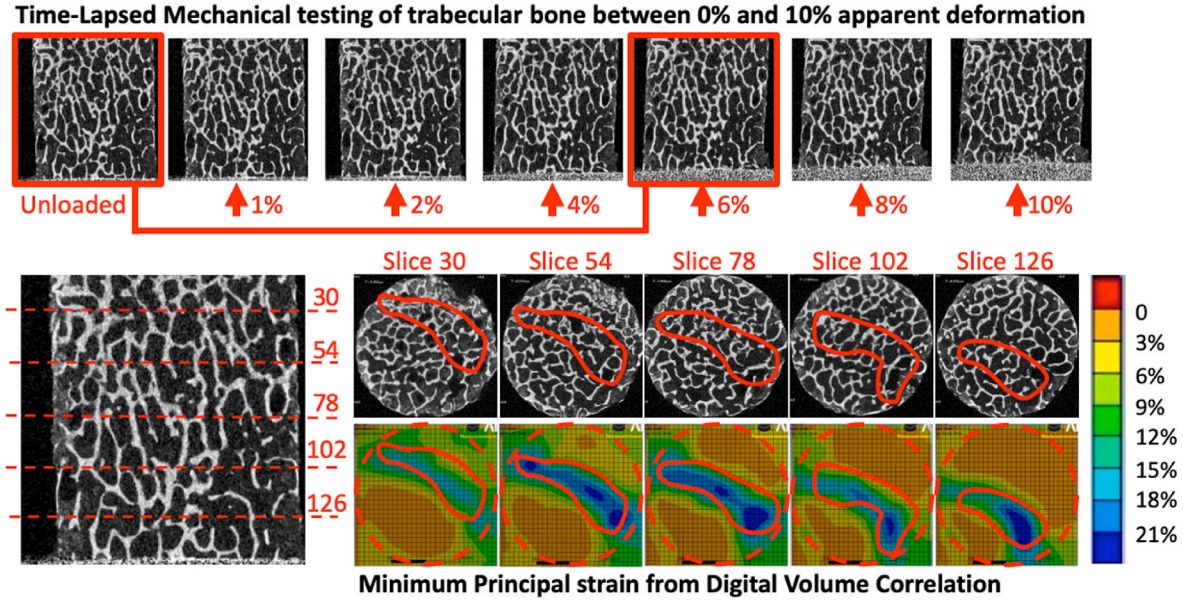

Fig. 1. Top: Time-lapsed compression of a cylindrical trabecular bone specimen until 10% apparent deformation, measured from images from a desktop microCT scanner (Skyscan 1172, Bruker; voxel size 34.44 μm). Bottom: Cross-sections of the specimen loaded until 6% apparent deformation and Minimum (Compressive) Principal Strain maps evaluated with Digital Volume Correlation (Nodal Spacing equal to ~500 μm) (Chen et al., 2017). The regions of failed trabeculae are outlined in red; these occur in highly strained regions (blue).

reconstructions (Lin et al., 2013), have been used to study the biomechanics of the rat bone-periodontal ligament-tooth joints.

While the potential of *in situ* microCT-based DVC analyses is recognised, limitation in the assessment of deformation for complex hierarchical biological structures are driven by the inevitable low resolution of the input desktop microCT images, which can resolve only features in the order of tens of micrometers in a reasonable time. While high resolution can be reached using the new generation of desktop microCT that use hardware similar to the Synchrotron (with lower flux), the time constraint related to the acquisition of each image (hours) limits their application for *in situ* mechanics. Nevertheless, some examples have recently been presented, including alveolar bone (Jang et al., 2021), cortical bone (Karali et al., 2021), rat bone (Karali et al., 2020) and bone-screw interface (Le Cann, Tudisco et al., 2020). For this reason, the combination of *in situ* mechanical testing and SR-microCT imaging was developed to improve the assessment of multi-scale deformation within biological tissues. The application of this approach to bone tissue was first undertaken by Thurner et al. (Thurner et al., 2006), who evaluated microdamage in bovine trabecular bone specimens tested in compression and showed that in most cases the failure mode of these structures is through delamination. High-resolution time-lapsed assessment of microcrack formation and propagation in cortical bone extracted from mouse femurs also highlighted how ultrastructure plays a fundamental role in bone fracture (Voide et al., 2009). More recently, this approach has been used to compare the failure mechanism of different bone specimens and analogous materials (Pena Fernandez, Kao et al., 2021). At a higher dimensional level, whole proximal femora have been tested in order to evaluate the link between failure mechanisms of bone and its heterogeneous microstructure (Martelli and Perilli, 2018). Similar approaches have been used to characterize the porosity and failure mechanisms in scaffolds for biomechanical applications (Charles-Harris, del Valle et al., 2007; Dhillon et al., 2011), to evaluate the integration of injectable biomaterials with tissue after implantation in animals (Yue et al., 2010, Pena Fernandez, Dall'Ara et al. 2019), or to test the mechanical properties of tissue and implanted screws (Le Cann, Tudisco et al., 2018).

One drawback to keep in mind and monitor closely, is the possible detrimental effect of radiation on mechanical properties. Prolonged exposure to high radiation doses alters bone bending stiffness and fracture toughness primarily by affecting its collagen cross-linking (Barth et al., 2010; Barth et al., 2011). In earlier experiments we have observed that repeated scanning at high resolution have caused cracks in the mineralised extracellular matrix of cortical (section 3.1) and trabecular (section 3.2) bone. However, failure mechanisms were not assessed in these studies, limiting the generalisation of their findings.

The highest potential of *in situ* mechanical testing and SR-microCT is achieved when combined with DVC to enable detailed analyses of local displacement and strain distributions. The superior efficiency and spatial resolution of SR-microCT images allow for visualization of features that are not resolved in standard desktop microCT scanners; this has reduced uncertainties in DVC calculations, which is fundamental to accurately assess local deformations and tissue failure (Palanca et al., 2017; Comini et al., 2019). The first application of SR-microCT-based DVC for assessing bone failure was performed by Christen et al. (Christen et al., 2012) who investigated crack propagation in cortical bone specimens extracted from a mouse femur and showed a relationship between micro-porosity, crack propagation and local deformation. Moreover, a recent study has shown how this technique can be used to study, at high resolution, strains within the subchondral bone of whole mouse knee joints loaded under compression, showing new mechanisms of deformation in the calcified cartilage and subchondral bone which are fundamental for better understanding the effect of diseases such as osteoarthritis on bone degeneration (Madi et al., 2020). The combination of SR-microCT imaging and DVC has been used to study trabecular bone damage (Turunen et al., 2020) and fracture toughness (Yan et al., 2020), to identify the best integration between bone grafts and bone tissue from detailed analyses of strain in the different subregions of the tested specimens (Pena Fernandez, Dall'Ara et al., 2019; Kok et al., 2022), and to evaluate deformation in the whole proximal femur (Martelli et al., 2021). Finally, to the authors' knowledge only one study has so far presented *in situ* SR-microCT measurements and DVC on soft tissues from the musculoskeletal system. Disney et al. (Disney et al., 2019) used the approach to characterize the heterogeneous deformation of intact rat intervertebral discs under compression. In order to increase contrast in the unstained soft tissue and resolve features within the disc (especially fibers in the annulus fibrosus), inline phase contrast with high propagation distance was used. All the studies mentioned here provided new detailed measurements of the local three-dimensional deformation that the tissues undergo during loading; this has substantially helped bridging the gap between tissue and cell dimensional levels in the characterization of hierarchical musculoskeletal tissues. While these applications have enabled to push the research forward in fields such as biomechanics and mechanobiology it is surprising that such a small number of studies have been published to date. This is due to a number of reasons that will be thoroughly discussed in the coming sections. First and foremost, little is known about the effect of radiation from SR-microCT on the properties of the tissue or biomaterials, making it difficult to compensate for its effect on the measured deformation field and to interpret the results. While recent studies have analyzed the effect of SR-microCT radiation on trabecular bone (Pena Fernandez, Cipiccia et al., 2018) and tried to reduce it by reducing temperature in the *in situ* experiments (Pena Fernandez, Dall'Ara et al., 2018), further work is needed to identify the best compromise between image quality and damage from radiation - via either its ionising or heating effects. In the latter mentioned study two temperatures were investigated, room temperature (~23C) and 0C, with specimens in saline solution. The experimental findings were reported in terms of residual strain accumulated in the irradiated tissue, corresponding to microcrack development, and suggested that the environmental cooling had an overall beneficial effect on structural integrity. While it remains to be investigated whether the cooling affected the intrinsic mechanical response of bone, the study suggested temperature control as a viable way forward to reduce irradiation-induced degradation. Moreover, the challenges in the acquisition of beamtime, in planning and performing the experiment in a short and stressful situation, and the interpretation of the huge amount of data obtained, all lead to experiments with relatively low number of (successful) specimens imaged, making it more difficult to generalize the findings.

The goal of this paper is to highlight the potential and pitfalls in the design and execution of repeated SR-microCT imaging of musculoskeletal tissues for the assessment of their structural and mechanical properties. Via advice and guidelines for improving the success rate of such experiments, we aim to help the community to undertake impactful research more efficiently in years to come.

2. Overview of approaches for in situ testing at synchrotron facilities

2.1. Beamlines equipped for combined in situ testing and SR-microCT

Several beamlines around the world have been used for *in situ* SR-microCT of biological tissues. While this list may not be exhaustive, we list here the most known beamlines at the Synchrotron facilities where the reported studies have been performed:

- Advanced Photon Source (APS), USA;
- Australian Synchrotron, Imaging and Medical Beamline, Australia;
- Diamond Light Source (DLS), I13-2 and I12, UK;
- Elettra light source, Synchrotron Radiation for Medical Physics (SYRMEP) beamline, Italy;
- European Synchrotron Radiation Facility (ESRF), ID19 beamline, France;

- Swiss Light Source (SLS), The Paul Scherrer Institute, X02DA TOMCAT beamline, Switzerland;
- Super Photon ring-8 (Spring-8), Japan;

2.2. Beamtime application

Applications are made via calls for proposals, which synchrotron facilities typically issue twice a year. It is useful to discuss the project with a beamline scientist before submitting an application; this person can advise upon various aspects of the proposed work: appropriateness of technique for achieving scientific aims, suitability of beamline, sample preparation and storage, experimental design, choice of beamline equipment, choice and integration of *in situ* rigs, health and safety considerations, contingency planning, proposed analysis methods, etc. Explanation of why SR-microCT (rather than desktop microCT) is needed to solve the current scientific problem is useful. Applications are peer reviewed by a panel, and after the submission of the application it commonly takes 6–12 months before beamtimes occur. Peer review panels typically assess on the basis of technical feasibility and scientific impact. Beamtimes are typically 1–4 days in length and the team has access to the facility 24hrs a day. However, synchrotron experiments can be complicated, and single-day experiments carry the risk of failure in the event of problems relating to instruments, samples, software or experimental strategy.

2.3. Beamtime preparation

Successful beamtimes rely upon good planning. Once a beamtime is scheduled, a *local contact* is typically assigned to the *user group*. This local contact is a synchrotron scientist who will be the point of contact for the experiment. It is advisable to discuss the proposed work with the local contact well in advance of the beamtime; this person will be able to help with experimental planning and might be able to direct the users towards examples of similar experiments conducted previously at the beamline. Particularly useful are methods articles that discuss optimisation of experiments, e.g. (Strotton et al., 2018). It can be possible to arrange a visit to the beamline in advance of the experiment to test and integrate any equipment you plan to bring, and ensure that the experiment will be safe for both people and beamline apparatus. Considering that the team will use the facility 24hrs a day it is important that all members of the team are trained in advance about the logistics of the experiment and, when possible, try to replicate the experiments, or simplified versions of them, in advance (e.g. with a desktop microCT system) to troubleshoot possible challenges in sample preparation and experimental design (see Section 3.4).

2.4. Sample preparation

To evaluate and preserve the mechanical performance of tissues, chemical techniques often employed in biological tomography to reduce motion artifacts (i.e. fixatives, embedding media) and enhance soft tissue contrast (chemical stains) must be avoided. To compensate, methods must be employed to reduce motion during scanning (e.g. fast data acquisition, relaxation prior to imaging), and optical means (phase contrast) must be employed to visualise non-mineralised tissues. Excellent contrast can be generated for unstained tissues with inline phase contrast alone (e.g. (Disney et al., 2017; Pierantoni et al., 2021)). The high flux and coherence of synchrotron X-rays therefore makes them highly valuable for the type of *in situ* tomography discussed in this article. In order to achieve the best results, tissues should be harvested, prepared, preserved and mounted appropriately. For bone, fresh tissues should be collected and subjected to the minimum number of freeze-thaw cycles for specimen preparation and testing. As in most cases bone specimens will be subjected to stepwise compression, appropriate end-capping should be considered by trimming the ends of the specimen and embedding in endcaps to achieve a 2:1 (free length: diameter) aspect ratio, thereby reducing experimental artifacts (Zhao et al., 2018). For any SR-microCT experiment, it is vital to ensure specimens are kept frozen during travel to the synchrotron facility (e.g. thermic bag, dry ice) and immediately stored in freezers available at the beamline upon request (see previous section).

2.5. In situ mechanical testing

Appropriate mechanical testing procedures are essential to ensure reliable results during *in situ* SR-microCT experiments. In standard applications, the load is applied in a stepwise manner to allow time for imaging the tissue at different load levels. However, this approach limits the ability of studying the effect of the viscoelastic response of the tissue on the 3D deformation. In fact, the viscoelastic properties of the tissues are ignored and the specimen is left to relax before each scanning step (5–30 min depending on the tested tissue), to avoid image artifacts induced by local movements of the specimen during the scan. Recently *in situ* continuous (time-resolved) mechanical testing combined with SR-microCT has been proposed for measuring 4D deformation in bone and bone analogues, which have a strong viscoelastic behaviour (Pena Fernandez, Kao et al., 2021). The approach represents a step-change in capturing the time-dependant mechanics of biomaterials by fully characterising their local strain-damage relationship, but the technical challenge of achieving high spatial resolution imaging makes stepwise loading still the preferred choice for most applications. Commercially available or custom-made devices have been used to characterize the deformation of musculoskeletal tissues in combination with tomography. While it is not our goal to review the used designs, rigs for *in situ* mechanical testing have similar requirements and features. The specimen has to be fixed in the frame facilitating alignment, this can be done outside the rig or directly within the rig with special grips; A load sensor (usually axial but multiaxial sensors are preferable) should be added to measure the applied load during the mechanical test, the monitoring of the load at each load-step is fundamental to decide the load level and to start the scan after the specimen has properly relaxed (plateau in the load -time curve); A loading mechanism (manual or motorized) to apply the nominal load (for example a screw-ball joint mechanism is usually used for applying stepwise compressive loads); The frame around the specimen has to be as radio-lucent as possible to avoid loss of image quality and contrast; The specimen has to be scanned and mechanically tested in conditions as close as possible to those in vivo, therefore environmental chambers with specimens submerged in saline solution or kept hydrated during the experiment are preferable. Moreover, in some desktop microCT systems the scanning space is very limited and, therefore, ad hoc designs are needed to maximise the field of view. Irrespective of whether a loading device has been commercially or custom made it is essential to perform a number of experiments offline in advance of the beamtime. These are typically meant to assess the stiffness/compliance of the moving parts and load readings by using a material with known mechanical properties (e.g. a synthetic foam) and subjecting it to the same stepwise testing regime to be used for the tissues (i.e. % of compression) to record the load-displacement curves and force fluctuation. Ideally, the results from the loading device should be compared to those from an equivalent specimen tested using a conventional (and more accurate) testing machine with the same (or similar) load cell capacity and reading uncertainty. Stress relaxation time should be also chosen beforehand in order to minimise movement artifacts during consecutive SR-microCT acquisitions. This is of increasing importance when going from hard to soft biomaterials and for high resolution images.

In order to preserve tissue integrity during *in situ* SR-microCT experiments, temperature control can be beneficial. Reducing the temperature of the saline solution in which the specimen is submerged (i.e. down to near 0 °C) can better preserve the structural integrity of tissues during irradiation (Pena Fernandez, Dall'Ara et al., 2018). Temperature control is currently available as additional option in some commercial

rigs (e.g. CT5000, Deben UK).

It is essential to ensure that the loading device is of a size compatible with the beamline; this should be discussed with beamline scientists before the experiment (see previous section). It is important to check that the field of view (FOV) is sufficient to image the specimen during all steps of *in situ* loading.

2.6. Tomographic scanning parameters

Given the importance of high-speed imaging for reducing deformations during imaging, experiments involving jointed limbs or flexible soft tissues must be conducted with a high flux beam. This can be either a pseudo-monochromatic beam (from a multilayer monochromator, or a combination of high- and low-pass transmission and reflective filters) or a pink (broad spectrum) beam. To limit radiation damage, the latter may be heavily filtered to suppress lower energy photons (<25 keV), which will be more readily absorbed by the sample.

Tomographic scanning parameters must be chosen so as to balance the various factors that determine spatial resolution (signal to noise ratio, contrast, blurring from Fresnel fringes, bulk/internal movements during scanning, etc.), while ensuring that sufficient loading steps are incorporated and mechanical properties are not unreasonably compromised by the radiation (see Section 2.7 and 3). For very stable samples, one would normally choose a large number of projection images to give a high signal to noise ratio (Strotton et al., 2018), but for *in situ* studies, this will unfortunately degrade both resolution (via sample deformation) and mechanical properties of the specimen (via collagen cross-linking).

Sample deformation and movement during tomographic data acquisition degrade resolution, and soft biological tissues or jointed limbs – particularly those under load – are very prone to motion. Such deformations can be assessed via comparison of images collected at the start (0°) and end (180°) of a 180° scan (see examples in Supplementary Figures of (Atwood et al., 2015)). Internal sample movements of say, 5 μm during data acquisition can easily thwart the aim of resolving 2 μm features, for example. Effective methods to deal with this problem include fast data acquisition (lower exposure time, lower number of projection images, a camera with a short overhead per image), custom-designed mounting and gripping of samples and short relaxation periods after loading before imaging is initiated.

The extent of inline phase-contrast is determined by the propagation distance between the sample and scintillator. A compromise must be found which will give good contrast (important for resolution) without allowing resolution to be degraded too much by strong Fresnel fringes. Any degradation of resolution will limit DVC precision. For bone, this means using the minimum propagation distance, whereas for soft tissues, larger distances must be employed. The appropriate distance depends upon both feature sizes and refractive index differences between neighbouring materials. For complex biological materials it is thus best determined empirically.

2.7. Considerations about radiation dose and dose calculation

In light of the sensitivity of collagen to radiation damage, and the effect this has on mechanical properties, Barth et al. (Barth et al., 2011) established a 'safe' radiation dose of 35 kGy based upon assessment of the mechanical properties of different groups of human cortical bone specimens that were subjected to different levels of radiation at a variety of synchrotrons and then mechanically tested. Given the error bars in flux/dose measurements/calculations, and given that it may be possible to reduce radiation damage by cooling the different tissues, this value should be considered as a guideline. Safe limits for a particular experimental setup should be established empirically (more details in Sections 3 and 4). The cumulative radiation induced to the specimen can be estimated by using simple considerations about the properties of the specimen and the scanning parameters. While the detailed procedures to estimate the radiation dose on the specimens are presented elsewhere ((Lovric et al., 2013) and supplementary material in (Pena Fernandez, Cipiccia et al., 2018)), it is fundamental for every new experiment to note the following parameters that are required to estimate, even retrospectively, the total absorbed radiation dose: Scanning parameters including beam type (monochromatic or polychromatic), beam energy, ID gap, beam filters, total exposure time; Sample parameters including shape, thickness, chemical composition and density (that will affect the X-Rays absorption).

2.8. Tomographic reconstruction and artefact correction

Two-dimensional projection images are reconstructed to three-dimensional tomograms via filtered back projection. If one performed a high number of scans on a single sample, dose limitations might result in noisy tomograms; iterative reconstruction methods could be considered in this instance. Reconstruction pipelines provide the opportunity to correct for artifacts that arise from experimental defects. These should of course be minimised at the experimental stage, but some are unavoidable. Some reconstruction pipelines are modular, and allow considerable flexibility in both the modules that may be incorporated and the choice of parameters that affect artefact removal (e.g. (Atwood et al., 2015; Basham et al., 2015)). With parallel computing, reconstruction usually takes a few minutes (Wadeson et al., 2016).

Ring artifacts arise from defects in the imaging system (particularly scintillators), and can seriously compromise subsequent analyses if not avoided experimentally or corrected for in software. DVC analysis relies upon textures and gradients of local grey-levels (attenuation) and may be particularly affected by ring artifacts. Various methods exist for suppressing these, and the chosen method and parameters should be dependent upon the nature of the defects (Vo et al., 2018). Zingers arise from stray X-rays directly striking the camera's detector chip, resulting in streaks in tomographic slices. When highly-scattering components of rigs (e.g. metals) are in the beam path, zingers can present a major problem. Methods for correcting zingers exist and, with correct parameter tuning, are highly effective (Fig. 2).

Images are collected with a detector coupled to a visual light microscope. Correction for the optical distortions (Vo et al., 2015) inherent in any such microscope can make significant improvements to data accuracy, and thereby the true resolution of data. Crucially, data accuracy can be substantially compromised by such distortions without the presentation of obvious artifacts – without the experimenter realizing there is anything wrong.

2.9. Data storage, handling, transfer

Tomographic datasets are very large. Each reconstruction generated at 32bit will be tens of GB in size, and tens or hundreds of those might be generated during a beamtime. It is therefore common that more than 10 TB data is generated in a beamtime, especially when *in situ* mechanical testing with repeated acquisitions for each specimen are performed. Handling such data volumes presents challenges relating to storage, transfer and analysis. It is possible for tens of TB of data to be generated that will ultimately prove impractical; for example, this can occur in experiments with different reconstruction strategies or when files relating to intermediate steps of a reconstruction pipeline are saved. Thus, tidying up disk space prior to data archiving can ease future workload considerably. It can also be useful to reduce the bit depths of reconstructions to reduce file size. A reduction of 32 to 16 or 8bit will reduce file size by a factor of 2 or 4, respectively, and is reasonable given that detectors are typically 16bit or less. One must be careful that significant information is not lost in this process; careful attention should be paid to lower and upper grey-level limits.

Data are typically archived by a synchrotron facility, and increasingly made available to the public some years after the experiment. Research groups are advised to take their own copies of data, and this is

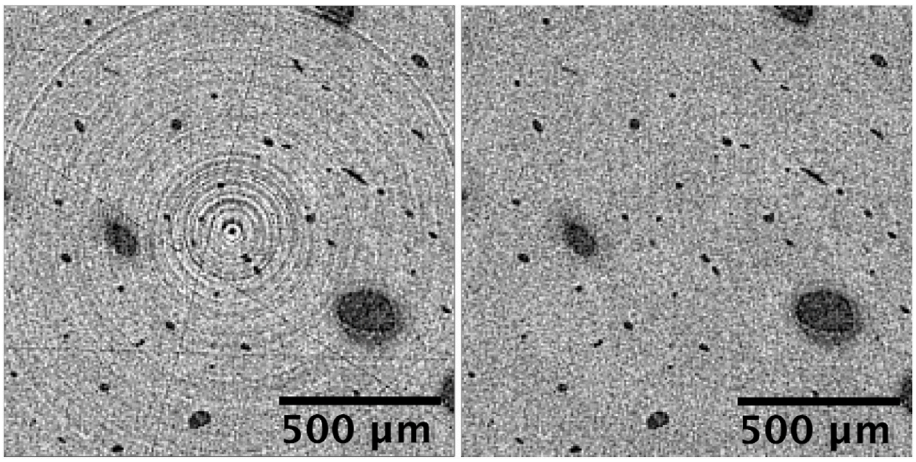

Fig. 2. Tomographic slice of cortical bone reconstructed without (left) and with (right) ring artiftact suppression and zinger removal. Note that the zingers in this example were particularly pronounced because X-rays were scattered from the compression rig. Data collected at Diamond Light Source (I13-2, MG22575-1).

typically done by transfer to portable hard-drives or via FTP.

Analysing large datasets can be a challenge, and expensive hardware and software can be required. Researchers might consider use of a 'data beamline' (Bodey and Rau, 2017) for their analyses; such facilities are typically equipped with high-powered workstations, access to computing clusters, and licenses for software packages that might be prohibitively expensive at some home institutions. Users might physically visit a synchrotron for data beamtimes, with arrangements handled in a similar way to an experimental beamtime.

2.10. Image post-processing and digital volume correlation

Noise in the images can be reduced by applying 3D filters (e.g. median, mean, Gaussian smoothing, Wiener). The choice of filters should be made by considering the trade-off between local smoothing with noise reduction and preservation of details and texture in the images. Edge-preserving filters (e.g. non-local means, Laplacian, unsharp) can reduce noise very effectively, but parameters must be chosen subjectively; the user must make a judgement call about what is considered noise and what is considered signal. To avoid biasing datasets, one might therefore avoid such filters or test their impact on the final outcomes of the experiment using benchmark dataset (e.g. the morphological properties of the tissue or the displacement and strain measurements from the DVC algorithm). Tomograms can be masked by setting the grey-scale intensity of the non-tissue/biomaterial voxels to zero. In order to achieve this, binary images must be generated in a process known as segmentation. However, due to the low exposure used during image acquisition to minimise irradiation-induced damage in the tissue, signal to noise can be low; Therefore, a global thresholding alone may be insufficient for segmenting tissue from the background. In order to improve segmentation, a global threshold can be followed by a combination of image processing methods (e.g. connectivity, erosion, dilation, filling, despeckling). Iterating these methods are recommended for best results, stopping the iterative process when no further improvements are observed. Masked images (with the original grey-scale value in the tissue/biomaterial and zero elsewhere) can be obtained by multiplying the original image with the binary image.

In order to allow a reliable DVC computation, a few preliminary steps must be followed. The SR-microCT tomograms for each specimen have to be rigidly registered and this can be done using rigid registration software (e.g. Fiji or Amira/Avizo from ThermoFisher Scientific) that finds the rigid transformation to match the target to the reference image. It should be noted that in case large deformations have been applied, it may be beneficial to find the rigid transformation based on rigid registration of a sub-portion of the image that has been minimally affected by the deformation. The optimised transformation can be then applied to the target image using interpolation (e.g. cubic spline). After registration, typically a volume of interest (VOI) for the analysis is cropped for each tomogram (e.g. parallelepiped, cube) and set in the centre of the tissue/biomaterial.

There are a number of DVC algorithms that can be used to study the deformation in tissues and biomaterials but their description is beyond the scope of this manuscript. Irrespective of the nature of DVC (local or global approach), it is mandatory to perform an error analysis to evaluate displacement/strain uncertainties in relation to the nature of the tissue/biomaterial under examination (Dall'Ara, Peña-Fernández et al., 2016). In order to account for image noise, uncertainties are typically evaluated by applying the DVC algorithm to two consecutive SR-microCT tomograms with no load (or a small preload applied *in situ*) to study a zero-strain (or constant-strain) case (Palanca et al., 2017). Recently synthetic deformation applied to repeated images has been proposed to evaluate the uncertainties under a known (simplified) deformation (Comini et al., 2019). However, given the damage in the collagen by the high flux synchrotron light, this must be carefully evaluated in the experimental planning by allowing an appropriate number of *in situ* loading steps, which would not exceed a critical accumulated dose. Finally, DVC can be computed and displacement/-strain reading visualized by overlaying the maps onto the structural features of the image. It must be noted that for materials with high porosity as trabecular bone, there is a difference between accurate measurements of the displacements/strains within each feature of the specimen (i.e. trabecula) and visualized values through interpolation. Measurements at the "tissue level" can be performed with DVC sub-volumes small enough to be included in the considered tissue. If instead DVC is using bigger sub-volumes to inscribe the tissue (i.e. larger than the trabeculae), the measurement should be referred to as at 'apparent level' (meso-scale) and the visualization of the displacement/strain maps onto the tissue will be affected by interpolation and may not be accurate.

3. Examples to highlight typical pitfalls

We share here three examples of negative results obtained when designing new *in situ* mechanical testing at synchrotron facilities for bone tissue. We hope that sharing these examples will help the inexperienced readers to avoid similar issues in future beamtimes and properly plan their experiments. In the first example we show how basic experiments can fail due to the wrong scanning condition or set of scanning parameters for SR-microCT imaging of cortical bone specimens. In the second example we show how scanning parameters can be optimised to

find a suitable compromise between image quality and trabecular bone tissue integrity. In the third example we show the extreme detrimental effects that radiation damage can have on the mechanical response of trabecular bone, and how one can use twin-samples to test the response with and without radiation to ensure that the damage is kept at a reasonable level.

3.1. Imaging of cortical bone, damage induced by SR-microCT imaging

The original objective of this study was to evaluate the local deformation in cortical bone specimens under compressive loading combining high resolution SR-microCT imaging, stepwise loading and DVC analyses. Nevertheless, a considerable amount of beamtime allocated for this experiment was lost due to the unexpected damage induced to the specimens during the scanning, that prevented us from assessing the local deformation of the specimens under load.

Cylindrical cortical bone specimens (3 mm in diameter) from the diaphysis of a bovine femur were SR-microCT images at DLS (I13-2 beamline). A filtered (950 μm C, 2 mm Al, 20 μm Ni) polychromatic 'pink' beam (5–35 keV) of parallel geometry was used with an undulator gap of 5 mm. Data were acquired using a pco.4000 detector (PCO AG, Germany) coupled to a 750 μm-thick CdWO4 scintillator, with visual optics providing 4X total magnification (effective pixel size of 2.25 μm and a FOV of 9.0 $\times$ 6.0 mm^2) and with a propagation distance of approximately 10 mm 2000 projections were collected at equally-spaced angles over 180 of continuous rotation, with an exposure time of 50 ms. The total scanning time was approximately 15 min. The projection images were flat and dark corrected prior to reconstruction using Dawn v1.7, which incorporated ring artefact suppression (Titarenko et al., 2010; Basham et al., 2015). The scans of two specimens extracted adjacent from each other are shown in this example. Both specimens were hydrated in 0.9% NaCl solution for 1 h before scanning. Specimen1 was mounted on a custom-made loading device (Chen et al., 2017) and scanned; Specimen2 was mounted in the same loading device with a liquid chamber containing 0.9%NaCl and scanned in solution.

The tomograms obtained with the scanning procedure showed good signal to noise ratio, that enabled the identification of different microporosities such as Haversian systems, smaller vessels typical of plexiform bones, a dense network of osteocyte lacunae (Fig. 3, right). However, in the bone specimen scanned hydrated in air (Specimen1) radial cracks, probably developed from the edge of the specimen, appeared after scanning, making the specimens unusable for further mechanical testing (Fig. 3, left). Conversely, in the bone specimen scanned in 0.9% NaCl solution (Specimen2) no cracks were visible after scanning with the same parameters. These specimens were not mechanically tested during the beamtime session as planned, to avoid inducing potential damage in the bone with repeated scans during the stepwise loading procedure. The specimens were transferred to a standard desktop microCT for further mechanical analyses. However, the specimens scanned as Specimen2 failed unexpectedly under a very low preload (~10N), probably due to diffuse damage not visible in the SR-microCT images that affected the specimen's mechanical integrity. These negative results motivated further studies to evaluate the effect of the SR-microCT imaging on the mechanical integrity of bone specimens. After the study the cumulative radiation dose has been calculated as 138.33 kGy for Specimen1 and 69.16 kGy for Specimen2, confirming that the radiation levels for both types of acquisitions were above the 'safe' radiation dose threshold recommended to avoid damage to collagen in bone (35 kGy) (Barth et al., 2011).

3.2. Repeated imaging of trabecular bone-biomaterial interface

This experiment aimed at understanding the local mechanical competence of ex vivo bone-biomaterial systems produced by four different bioresorbable grafts implanted in an ovine animal model, using *in situ* SR-microCT and DVC. Nevertheless, a considerable amount of beamtime allocated for this experiment was used to optimise the imaging parameters in order to obtain image quality high enough for

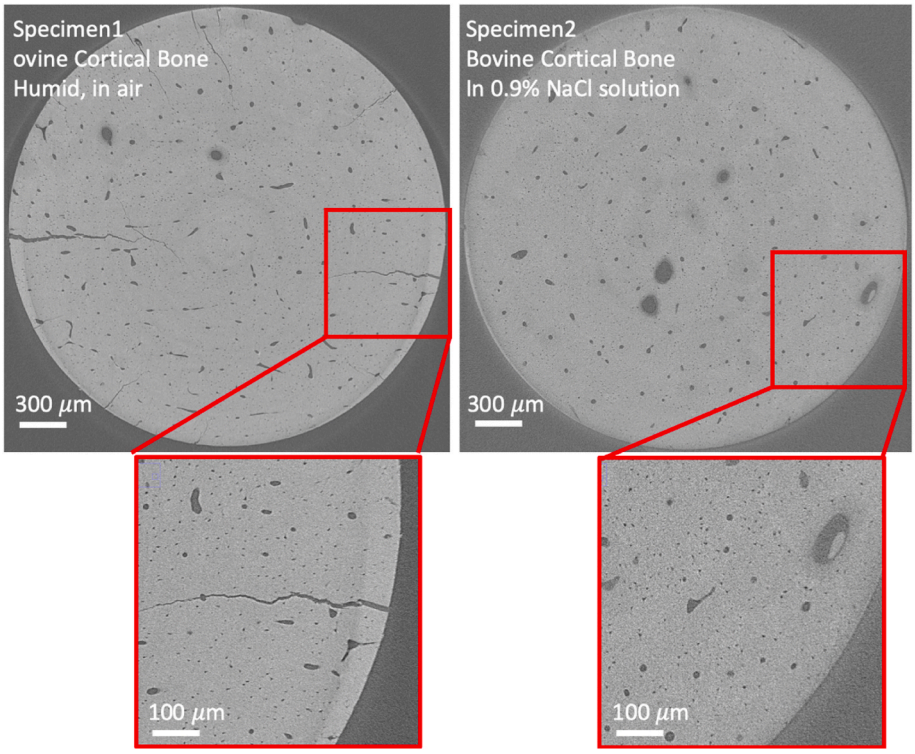

Fig. 3. *Example of cross-sectional images of bovine cortical bone cylindrical specimens (3 mm in diameter) scanned with SR-microCT (voxel size 2.25 μm) humid in air (Specimen1) or submerged in 0.9% NaCl solution in a liquid chamber (Specimen2). The specimen scanned in air exhibited clear radial cracks after scanning. The two specimens were extracted from adjacent locations of the same bone tissue. Data collected at DLS (I13-2, MT10315-1).*

subsequent DVC analysis and at the same time preserving as much as possible the mechanical integrity of bone tissue.

An ovine bone-biomaterial (ApaPore) cylinder (4 mm in diameter) from implanted femoral condyles was used, following Ethics approval granted by the Royal Veterinary College and in compliance with the United Kingdom Home Office regulations (Animal Scientific Procedures Act [1986]).

SR-microCT imaging was performed at DLS (I13–2, MT14080-1), using a filtered (1.3 mm pyrolytic graphite, 3.2 mm aluminium and 60 μm steel) partially-coherent polychromatic 'pink' beam (5–35 keV) of parallel geometry with an undulator gap of 5 mm. Projections were recorded by a sCMOS (2560 × 2160pixels) pco.edge 5.5 (PCO AG, Germany) detector, which was coupled to a 500 μm-thick CdWO4 and a visual light microscope. A 1.25X objective lens was used to achieve a total magnification of 2.5X, resulting in effective voxel size of 2.6 μm and a FOV of 6.7 × 5.6 mm^2. For each dataset, projections were collected over 180 degrees of continuous rotation ('fly scan'). The final projection was not used for reconstruction, but was compared to the first image to check for experimental problems including sample deformation and bulk movements. The propagation distance (sample to detector) was set to 50 mm allowing sufficient in-line phase-contrast to visualise the microstructure and projection images were flat-field and dark-field corrected prior to reconstruction. Reconstruction was performed at DLS using the in-house software, Dawn, incorporating ring artefact suppression. Acquisition parameters including nominal exposure time per projection (the nominal time may be subjected to some variation due to the readout time associated to the used detector), number of projections, time of single tomography, cumulative time, and cumulative calculated dose for the ten consecutive tomograms of the experiment are reported in Table 1 (details of the dose calculation in the supplementary material of (Pena Fernandez, Cipiccia et al., 2018)).

As shown in Fig. 4 the improvement in image contrast by increasing exposure time led to the development of large microcracks within both pre-existing and newly formed trabecular bone (Fig. 4 C and D). This result highlighted the need of further imaging on site to determine reasonable conditions to perform the planned and original *in situ* SR-microCT experiment.

3.3. Imaging of trabecular bone

This study aimed to determine trabecular strain evolution during loading of human bone from donors of varying age and health status. The goal was to obtain high enough image resolution and quality to enable DVC calculations with a resulting spatial resolution for strain measurement at the sub-trabecular level. Furthermore, the study attempted to load the samples continuously at a slow rate, to avoid relaxation times and enable more detailed information on the yield transition and post-yield behaviour. Thus, very fast image acquisition was a requirement.

Table 1
Nominal acquisition parameters and calculated dose for ten consecutive acquisitions on the same bone-biomaterial specimen. The cumulative dose should be considered to avoid performing analyses on specimens damaged by the radiation.

Exposure time [s]	Projections [.]	Tomography time [s]	Cumulative time [s]	Cumulative dose [kGy]
0.01	401	4.0	4.0	0.1
0.01	4001	40.0	44.0	1.5
0.016	1801	28.8	72.8	2.6
0.032	1801	57.6	130.5	4.6
0.064	1801	115.3	245.7	8.6
0.128	1801	230.5	476.3	16.7
0.256	1801	461.1	937.3	32.8
0.512	1801	922.1	1859.4	65.1
1.024	1801	1844.2	3703.7	129.6
1.024	1801	1844.2	5547.9	194.2

Human trabecular bone plugs were obtained with permission (National Authority for Medicolegal Affairs, TEO, 5783/04/044/07) from the femoral neck/head junction. Several sequential bone plugs were extracted from each donor to create 'twin-like' samples with minimal variation. The experiment was carried out at the SLS (X02DA TOMCAT beamline). The samples were placed inside a polycarbonate tube of a custom-made loading rig (Fig. 5A). To enable fast imaging that would allow continuous loading, a polychromatic white beam was used. The giga-FROST detector was used with a FOV of 2016×2016 pixels (~7.3×7.3 mm^2), voxel size 3.6 μm, exposure time of 3.5 ms. Resulting imaging times were ~6s for a full tomography dataset with good enough image quality to perform DVC. A low continuous loading rate of 0.05 mm/min was used to ensure that the loading speed was less than two pixels displacement during one scan.

Unfortunately, during *in situ* testing, it became clear that the radiation imposed by the imaging was diminishing the bone tissues ability to resist load (Fig. 5B, red). To ensure it was not an issue related with the specific samples or with the loading device, twin samples were loaded without imaging (no radiation), presenting the expected load-response (Fig. 5B, blue). Despite minimizing exposure during setup and alignment and the number of scans, the detrimental effects remained. During setup, testing and troubleshooting, in total 8 specimens were lost and roughly 24 h of beamtime.

The setup was changed, and instead a monochromatic X-ray beam with an energy of 30 keV was used, with a high-speed CMOS (Complementary Metal Oxide Semiconductor) detector (pco.Dimax) coupled to visible-light optics with a 100 μm thick scintillator (LuAg:Ce). A full tomographic dataset was acquired in 45s, by keeping the intended resolution (voxel size of 3.6 μm). Samples were compressed step-wise instead of continuously to minimise movement artifacts. The procedure was repeated until fracture, resulting in a total of 4–9 scans/steps per sample. The sample was placed wet in a closed loading container during the measurement protocol, which lasted up to 25 min (depending on the number of scans). No significant dehydration was observed. A dose model was adopted to estimate the absorbed dose for each scan (Lovric et al., 2013), which ranged between 17 kGy and 28 kGy, mainly depending on the total number of scans per sample. No systematic differences in mechanical behaviour were observed between the *in situ* tested samples, and the twin samples tested afterwards without radiation (Fig. 5C, red and blue). The full description and data are available in (Turunen et al., 2020).

3.4. Take home message from these experiments

All three studies failed due to the effect of SR-microCT imaging on the mechanical integrity of bone specimens. In order to minimise the potential tissue damage, it is recommended that radiation dose is assessed from flux measurements or simulations, even though both have uncertainties. The 35 kGy threshold proposed in previous literature for cortical bone imaging (Barth et al., 2010) might serve as a useful guide to avoid damage and design the acquisition setup and parameters. Nevertheless, it is best to empirically establish a safe limit for given setup and specimens in order to find the best compromise between radiation dose and image quality, which will affect the uncertainties of further analyses (e.g. DVC analysis). This can be achieved with the assessment of mechanical properties of the specimens before and after scanning, to identify possible degradation in mechanical integrity and plan potential solutions. For example, cooling seems to be protective from tissue degradation (Pena Fernandez, Dall'Ara et al., 2018). However, the latter study only aimed to assess the effect of environmental conditions in irradiation-induced damage of bone tissue by coupling microcrack detection and DVC residual strain during the experiment. Thus, further analysis is needed to properly assess the effect of the environmental temperature during *in situ* SR-microCT mechanics.

All these typical beginner mistakes could have been solved with more detailed planning and knowledge about the effect of the different

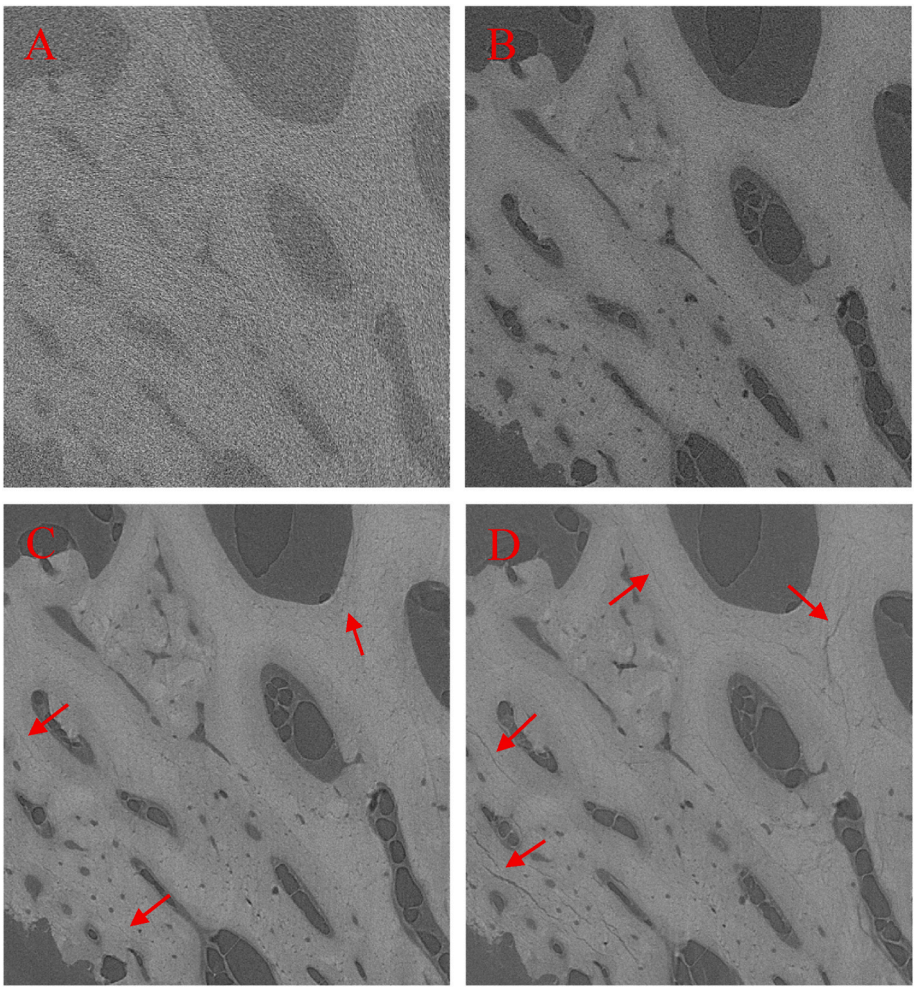

Fig. 4. SR-microCT images of ovine bone-biomaterial ex vivo acquired with different exposure times. Red arrows indicate the radiation damage induced in the bone. A) t_{exp} = 16 ms. Δt_{exp} = 72.84 s. B) t_{exp} = 128 ms. Δt_{exp} = 476.26 s. C) t_{exp} = 1024 ms. Δt_{exp} = 3703.65 s. D) t_{exp} = 1024 ms. Δt_{exp} = 5547.88 s (t_{exp}: exposure time; Δt_{exp}: cumulative exposure time). Data collected at Diamond Light Source (I13–2, MT14080-1).

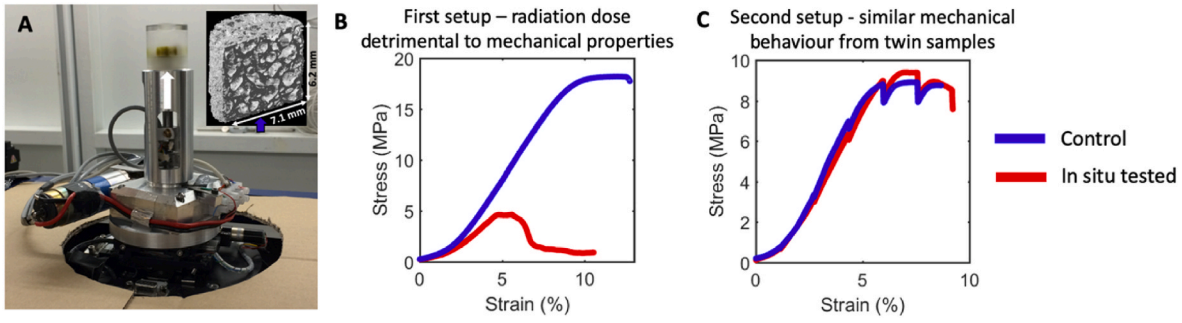

Fig. 5. *A) Loading rig with polycarbonate tube surrounding the sample (left). B) The first setup with polychromatic beam and continuous in situ loading/scanning clearly reduced the bone tissues mechanical response (middle) exemplified by one set of twin samples. C) The second setup with monochromatic beam and sequential load steps followed by imaging resulted in highly similar mechanical response, exemplified by one set of twin samples. Blue refers to samples only tested mechanically (without imaging), whereas red refers to samples that were in situ tested (imaged and mechanical testing). Data collected at Swiss Light Source (TOMCAT, 20150257), and outcome from C is available in* (Turunen et al., 2020).

decisions during setup on the effective radiation dose. Another important lesson learnt during these experiments was to always have a substantial number of extra samples at hand, and that the use of biological 'twin' samples to test mechanical behaviour within and outside of the beam is a good idea when testing a new tissue type, imaging setup or beamline. Better experimental planning, in depth discussion with beamline scientists, and rough estimation of radiation doses beforehand would have saved several shifts of beamtime. Finally, it is crucial to be aware of the expected range in mechanical response from extensive previous testing before arriving at the beamline. Some of the most common issues associated with experiments involving *in situ* mechanical testing and SR-microCT imaging and advice to minimise their impact are summarised in Table 2.

Table 2
Most common issues to consider before, during and after experiments involving *in situ* mechanical testing and SR-microCT imaging and advice to minimise them.

Stage	Issue	Suggestions
Experiment planning	Setting up the scanning protocol is not easy and should be planned in advance	- Talk to the beamline scientist about the imaging, loading device, specimens and scientific aims. - Estimate radiation dose, bearing error bars in mind and any heatsinking or cooling. - Test your loading device extensively, and if possible at the beamline before the beamtime. - Check the literature for recommendations about potentially successful scanning procedures that could be replicated for your application.
Beamtime preparation	Beamtimes are time-limited	- Prepare the samples well in advance if possible, and bring spare samples. Things may go wrong; - Organise a trial session in the local laboratory to test timings for specimens that have to be prepared last minute at the laboratory at the Synchrotron facility; - Plan which team members will be responsible for the different tasks (sample preparation, acquisition, reconstructions, pre-processing) and which shifts they will work; - Make sure that all apparatus (loading device, sensors, external acquisition systems, sample holders, environmental chambers, etc.) has been tested and is working properly; - Ensure safe sample shipment.
Sample preparation	Sample preparation and storage at the facility may benefit from planning	- Evaluate what can be prepared before the beamtime and optimise the sample preparation procedure; - Contact the beamline scientist and the facility managers in advance to confirm access to laboratories for specimen preparation and storage (e.g. freezers for animal/human tissues); - Plan how the specimen will be positioned in the sample holders at the beamline.
Mechanical testing	Mechanical tests should be optimised for the environment of the beamline laboratories	- Consider how to integrate the loading device with the beamline and how to control it; - Test in advance potential interactions between the features of the rig and the beam (interference with sensors, damage to components, etc.); - Decide the environment of the specimen. Specimens generally should not be scanned in air and even for short scans in solution are preferred. If environmental chambers are available cooling of the specimens could be helpful to reduce the damage induced by potential temperature gradients.
Image acquisition	Choosing scanning parameters to find the best compromise between image quality, resolution and scanning time (and thereby radiation damage) is not trivial	- Effect of imaging parameters on the flux and radiation dose: certain scanning procedures may affect the mechanical properties of the scanned biological tissues, in particular for the repeated images required in in situ testing; - Optimise the scanning parameters based on previous experiments, literature research and dose estimates; - There are several parameters to that should be discussed with the beamline scientist prior to the beamtime.
Image reconstruction	Image artifacts may appear due to the hardware used; correction during reconstruction could be beneficial but has to be optimised.	- Evaluate image quality before starting with the mechanical testing; - Optimise hardware solutions (e.g. filters); - Make sure that you evaluate the reconstructed images before and after the corrections are applied.
Data storage and handling	A huge amount of data may be produced and time is needed to copy them before leaving the beamline.	- Bring enough hard-drives (several TB); - Tidy up disk space. Decide which files should be copied during the experiment so that they can be moved to external drives for first post-processing; - Reduce bitdepth when possible.
Image processing and analyses	The image processing and analyses should be optimised to be able to process large datasets	- Estimate in advance what steps are needed to process the images in order to identify the needed parameters. While this step usually requires examples of images from the session, the general planning could save time during the experiments (e.g. do you need 32/16/8 bit images? Can you process one load step or do you need more scans at different load steps?); - Identify any required software package that could improve the quality and efficiency of your pipeline for image processing. There may be software available at the beamline facilities to help with the process; - Estimate the time needed to process the data to avoid them sitting in the laboratory for several months/years.

4. Discussion and perspective

The goal of this paper was to describe the typical experiments performed in synchrotron facilities to characterize the morphology and mechanical properties of musculoskeletal tissues. The most common pitfalls in the experimental design, execution and interpretation of the results have been presented and, finally, advice and guidelines have been reported to help unexperienced researchers in developing their experiments.

The vast majority of experiments combining *in situ* mechanical testing and SR-microCT imaging have focused on the characterization of mineralised tissues, in particular bone. Nevertheless, most results presented in the literature are affected by experimental challenges related to the invasiveness of the SR-microCT imaging and its effect on the mechanical integrity of the tissue. In this area of research more effort should be invested in the optimisation of the scanning parameters and hardware to minimise the effect of the imaging on the mechanical properties and three-dimensional deformation of the tissue. This advancement should go hand in hand with the development and optimisation of DVC approaches to study the deformation of mineralised tissues. For example, considering that bone tissue yields at approximately 1% of deformation, in order to study its heterogeneous deformation in the elastic regime, high accuracy and precision of the DVC approach is required. High accuracy and precision can be achieved by increasing the resolution of the input images (Palanca et al., 2017; Comini et al., 2019), which however require longer scanning time and radiation, which seem to be directly related to the induced damage (Pena Fernandez, Cipiccia et al., 2018). Therefore, for each new experiment, time and resources should be allocated to find the best compromise between the image quality and the radiation-induced damage and/or to protect the specimens from by, for example, cooling the specimen in a temperature-controlled bath (Pena Fernandez, Dall'Ara et al., 2018) or reducing the scanning time with dynamic microCT (Dewanckele et al., 2020).

Recent advancements in SR-microCT phase-contrast imaging of native rodent soft tissues such as the intervertebral disc (Disney et al., 2019), growth plate (Pierantoni et al., 2021) and tendons (Pierantoni et al., 2021), have enabled to study their microstructure in 3D. However, only the study of the intervertebral disc included *in situ* loading and the images have been used to evaluate the deformation of the tissue under load with DVC (Disney et al., 2019). Therefore, future effort should be invested into understanding the effect of radiation on the mechanical integrity of soft tissues and understanding the relationship between mechanical and microstructural properties of these tissues. Furthermore, while at the moment SR-microCT facilities enable to scan at high resolution only a relatively small FOV, development and optimisation of hardware for acquisition, reconstruction and handling of large datasets are needed to characterize the properties of biological tissues. Finally, the assessment of the microstructural and mechanical properties of joints is fundamental to understand their degeneration in osteoarthritis, back pain, and other diseases. Nevertheless, the optimisation of the imaging and image processing of the joints, made of both hard and soft tissues, is challenging. Combination of absorption and phase-contrast imaging modalities could be used at the cost of increasing the scanning time (Tozzi et al., 2020), but if to be used for mechanical characterization more effort should be invested to evaluate the mechanical integrity of the tissues after scanning.

In order to compensate for the limited access to synchrotron facilities, high resolution desktop microCT scanners have been developed. With these machines excellent image resolution can be obtained, combinations of absorption and phase-contrast modalities is possible, and enough space is available between the X-ray source and detector to install loading devices for *in situ* mechanical testing. However, a longer scanning time compared to SR-microCT imaging is needed in order to compensate for the lower flux of the X-ray source. Unfortunately, little has been done to characterize the effect of the long scans on the mechanical properties of the tested tissues, although a recent study reported how prolonged X-ray exposure in microCT had an effect in reducing stiffness and hardness of articular cartilage (Tozzi et al., 2020). Therefore, as for SR-microCT imaging, future scanning protocols should be optimised to find the best compromise between the image quality and the potential damage induced to the specimens due to the radiation.

In this manuscript we have outlined typical pitfalls in the designing of experiments involving *in situ* mechanical testing and high-resolution microCT imaging and attempted to provide guidelines to reduce the number of unsuccessful experiments for musculoskeletal tissues as much as possible. Obviously, the approaches used in each experiment will be driven by the research question. Nevertheless, we hope that the guidelines reported here can help researchers who are planning to apply these approaches for the first time and help to standardise the reporting of the methods and results from studies where *in situ* mechanical testing and SR-microCT imaging have been used.

CRediT authorship contribution statement

E. Dall'Ara: Writing – review & editing, Writing – original draft, Visualization, Resources, Methodology, Investigation, Funding acquisition, Formal analysis, Data curation, Conceptualization. **A.J. Bodey:** Writing – review & editing, Writing – original draft, Visualization, Methodology, Investigation, Formal analysis, Data curation, Conceptualization. **H. Isaksson:** Writing – review & editing, Writing – original draft, Visualization, Resources, Methodology, Investigation, Funding acquisition, Formal analysis, Data curation, Conceptualization. **G. Tozzi:** Writing – review & editing, Writing – original draft, Visualization, Resources, Methodology, Investigation, Funding acquisition, Formal analysis, Data curation, Conceptualization.

Declaration of competing interest

The authors declare that they have no known competing financial interests or personal relationships that could have appeared to influence the work reported in this paper.

Acknowledgements

We acknowledge the Paul Scherrer Institut, Villigen, Switzerland for provision of synchrotron radiation beamtime at the TOMCAT beamline X02DA of the SLS (20150257) and Diamond Light Source for provision of synchrotron radiation beamtime at I13-2 (MT10315, MT16497-2, MG22575-1).

The authors gratefully acknowledge Dr Yuan Chen, Dr Andre Castro, Dr Ana Campos Marin, Dr Claudia Wittkowske and Dr Luke Boldock for the help during the experiments presented in section 3.1; Dr Marta Peña Fernández for the data presented in section 3.2; Dr. Mikael Turunen and Dr. Sophie Le Cann for the data and figure presented in section 3.3.

The study was partially funded by the EPSRC Frontier Grant Multisim (EP/K03877X/1 and EP/S032940/1), FP7 European program (MAMBO, PIEF-GA-2012-327357), the Knut and Alice Wallenberg KAW Foundation (Wallenberg Academy Fellows 2017.0221), and the European Research Council (ERC) under the European Union's Horizon 2020 research and innovation programme (grant agreement No 101002516).

References

Atwood, R.C., Bodey, A.J., Price, S.W., Basham, M., Drakopoulos, M., 2015. A high-throughput system for high-quality tomographic reconstruction of large datasets at Diamond Light Source. Philos. Trans. A Math Phys. Eng. Sci. 373, 2043.

Barth, H.D., Launey, M.E., Macdowell, A.A., Ager 3rd, J.W., Ritchie, R.O., 2010. On the effect of X-ray irradiation on the deformation and fracture behavior of human cortical bone. Bone 46 (6), 1475–1485.

Barth, H.D., Zimmermann, E.A., Schaible, E., Tang, S.Y., Alliston, T., Ritchie, R.O., 2011. Characterization of the effects of x-ray irradiation on the hierarchical structure and mechanical properties of human cortical bone. Biomaterials 32 (34), 8892–8904.

Basham, M., Filik, J., Wharmby, M.T., Chang, P.C., El Kassaby, B., Gerring, M., Aishima, J., Levik, K., Pulford, B.C., Sikharulidze, I., Sneddon, D., Webber, M., Dhesi, S.S., Maccherozzi, F., Svensson, O., Brockhauser, S., Naray, G., Ashton, A.W., 2015. Data analysis WorkbeNch (DAWN). J. Synchrotron Radiat. 22 (3), 853–858.

Bay, B.K., 1995. Texture correlation: a method for the measurement of detailed strain distributions within trabecular bone. J. Orthop. Res. 13 (2), 258–267.

Bergomi, M., Cugnoni, J., Wiskott, H.W., Schneider, P., Stampanoni, M., Botsis, J., Belser, U.C., 2010. Three-dimensional morphometry of strained bovine periodontal ligament using synchrotron radiation-based tomography. J. Anat. 217 (2), 126–134.

Bodey, A.J., Rau, C., 2017. Launch of the I13-2 data beamline at the Diamond light source synchrotron. J. Phys. Conf. 849, 012038.

Boulanaache, Y., Becce, F., Farron, A., Pioletti, D.P., Terrier, A., 2020. Glenoid bone strain after anatomical total shoulder arthroplasty: in vitro measurements with micro-CT and digital volume correlation. Med. Eng. Phys. 85, 48–54.
Charles-Harris, M., del Valle, S., Hentges, E., Bleuet, P., Lacroix, D., Planell, J.A., 2007. Mechanical and structural characterisation of completely degradable polylactic acid/calcium phosphate glass scaffolds. Biomaterials 28 (30), 4429–4438.
Chen, Y., Dall Ara, E., Sales, E., Manda, K., Wallace, R., Pankaj, P., Viceconti, M., 2017. Micro-CT based finite element models of cancellous bone predict accurately displacement once the boundary condition is well replicated: a validation study. J. Mech. Behav. Biomed. Mater. 65, 644–651.
Christen, D., Levchuk, A., Schori, S., Schneider, P., Boyd, S.K., Muller, R., 2012. Deformable image registration and 3D strain mapping for the quantitative assessment of cortical bone microdamage. J. Mech. Behav. Biomed. Mater. 8, 184–193.
Clark, J.N., Heyraud, A., Tavana, S., Al-Jabri, T., Tallia, F., Clark, B., Blunn, G.W., Cobb, J.P., Hansen, U., Jones, J.R., Jeffers, J.R.T., 2020. Exploratory full-field mechanical analysis across the osteochondral tissue-biomaterial interface in an ovine model. Materials 13 (18).
Clark, J.N., Tavana, S., Clark, B., Briggs, T., Jeffers, J.R.T., Hansen, U., 2021. High resolution three-dimensional strain measurements in human articular cartilage. J. Mech. Behav. Biomed. Mater. 124, 104806.
Coan, P., Bamberg, F., Diemoz, P.C., Bravin, A., Timpert, K., Mutzel, E., Raya, J.G., Adam-Neumair, S., Reiser, M.F., Glaser, C., 2010. Characterization of osteoarthritic and normal human patella cartilage by computed tomography X-ray phase-contrast imaging: a feasibility study. Invest. Radiol. 45 (7), 437–444.
Comini, F., Palanca, M., Cristofolini, L., Dall'Ara, E., 2019. Uncertainties of synchrotron microCT-based digital volume correlation bone strain measurements under simulated deformation. J. Biomech. 86, 232–237.
Costa, M.C., Tozzi, G., Cristofolini, L., Danesi, V., Viceconti, M., Dall'Ara, E., 2017. Micro Finite Element models of the vertebral body: validation of local displacement predictions. PLoS One 12 (7), e0180151.
Dall'Ara, E., Barber, D., Viceconti, M., 2014. About the inevitable compromise between spatial resolution and accuracy of strain measurement for bone tissue: a 3D zero-strain study. J. Biomech. 47 (12), 2956–2963.
Dall'Ara, E., Luisier, B., Schmidt, R., Kainberger, F., Zysset, P., Pahr, D., 2013. A nonlinear QCT-based finite element model validation study for the human femur tested in two configurations in vitro. Bone 52 (1), 27–38.
Dall'Ara, E., Peña-Fernández, M., Palanca, M., Giorgi, M., Cristofolini, L., Tozzi, G., 2016. Precision of digital volume correlation approaches for strain analysis in bone imaged with micro-computed tomography at different dimensional levels. Front. Mater 4 (31).
Danesi, V., Tozzi, G., Cristofolini, L., 2016. Application of digital volume correlation to study the efficacy of prophylactic vertebral augmentation. Clin. Biomech. 39, 14–24.
Dewanckele, J., Boone, M.A., Coppens, F., Van Loo, D., Merkle, A.P., 2020. Innovations in laboratory-based dynamic micro-CT to accelerate in situ research. J. Microsc. 277 (3), 197–209.
Dhillon, A., Schneider, P., Kuhn, G., Reinwald, Y., White, L.J., Levchuk, A., Rose, F.R., Muller, R., Shakesheff, K.M., Rahman, C.V., 2011. Analysis of sintered polymer scaffolds using concomitant synchrotron computed tomography and in situ mechanical testing. J. Mater. Sci. Mater. Med. 22 (12), 2599–2605.
Disney, C.M., Eckersley, A., McConnell, J.C., Geng, H., Bodey, A.J., Hoyland, J.A., Lee, P. D., Sherratt, M.J., Bay, B.K., 2019. Synchrotron tomography of intervertebral disc deformation quantified by digital volume correlation reveals microstructural influence on strain patterns. Acta Biomater. 92, 290–304.
Disney, C.M., Madi, K., Bodey, A.J., Lee, P.D., Hoyland, J.A., Sherratt, M.J., 2017. Visualising the 3D microstructure of stained and native intervertebral discs using X-ray microtomography. Sci. Rep. 7 (1), 16279.
Ehrenfried, L.M., Farrar, D., Cameron, R.E., 2010. The degradation properties of co-continuous calcium phosphate polyester composites: insights with synchrotron micro-computer tomography. J. R. Soc. Interface 7 (Suppl. 5), S663–S674.
Fu, Q., Huang, W., Jia, W., Rahaman, M.N., Liu, X., Tomsia, A.P., 2011. Three-dimensional visualization of bioactive glass-bone integration in a rabbit tibia model using synchrotron X-ray microcomputed tomography. Tissue Eng. 17 (23–24), 3077–3084.
Grassi, L., Isaksson, H., 2015. Extracting accurate strain measurements in bone mechanics: a critical review of current methods. J. Mech. Behav. Biomed. Mater. 50, 43–54.
Honkanen, M.K.M., Saukko, A.E.A., Turunen, M.J., Shaikh, R., Prakash, M., Lovric, G., Joukainen, A., Kroger, H., Grinstaff, M.W., Toyras, J., 2020. Synchrotron MicroCT reveals the potential of the dual contrast technique for quantitative assessment of human articular cartilage composition. J. Orthop. Res. 38 (3), 563–573.
Horng, A., Stroebel, J., Geith, T., Milz, S., Pacureanu, A., Yang, Y., Cloetens, P., Lovric, G., Mittone, A., Bravin, A., Coan, P., 2021. Multiscale X-ray phase contrast imaging of human cartilage for investigating osteoarthritis formation. J. Biomed. Sci. 28 (1), 42.
Hosseini, H.S., Clouthier, A.L., Zysset, P.K., 2014. Experimental validation of finite element analysis of human vertebral collapse under large compressive strains. J. Biomech. Eng. 136 (4).
Hussein, A.I., Louzeiro, D.T., Unnikrishnan, G.U., Morgan, E.F., 2018. Differences in trabecular microarchitecture and simplified boundary conditions limit the accuracy of quantitative computed tomography-based finite element models of vertebral failure. J. Biomech. Eng. 140 (2).
Jackman, T.M., Hussein, A.I., Curtiss, C., Fein, P.M., Camp, A., De Barros, L., Morgan, E. F., 2016. Quantitative, 3D visualization of the initiation and progression of vertebral fractures under compression and anterior flexion. J. Bone Miner. Res. 31 (4), 777–788.
Jang, A., Wang, B., Ustriyana, P., Gansky, S.A., Maslenikov, I., Useinov, A., Prevost, R., Ho, S.P., 2021. Functional adaptation of interradicular alveolar bone to reduced chewing loads on dentoalveolar joints in rats. Dent. Mater. 37 (3), 486–495.
Joffre, T., Isaksson, P., Procter, P., Persson, C., 2017. Trabecular deformations during screw pull-out: a micro-CT study of lapine bone. Biomech. Model. Mechanobiol. 16 (4), 1349–1359.
Karali, A., Kao, A.P., Meeson, R., Roldo, M., Blunn, G.W., Tozzi, G., 2020. Full-field strain of regenerated bone tissue in a femoral fracture model. J. Microsc. 285 (3), 156–166.
Karali, A., Kao, A.P., Zekonyte, J., Blunn, G., Tozzi, G., 2021. Micromechanical evaluation of cortical bone using in situ XCT indentation and digital volume correlation. J. Mech. Behav. Biomed. Mater. 115, 104298.
Knowles, N.K., Kusins, J., Faieghi, M., Ryan, M., Dall'Ara, E., Ferreira, L.M., 2019. Material mapping of QCT-derived scapular models: a comparison with micro-CT loaded specimens using digital volume correlation. Ann. Biomed. Eng. 47 (11), 2188–2198.
Kok, J., Tornquist, E., Raina, D.B., Le Cann, S., Novak, V., Sirka, A., Lidgren, L., Grassi, L., Isaksson, H., 2022. Fracture behavior of a composite of bone and calcium sulfate/hydroxyapatite. J. Mech. Behav. Biomed. Mater. 130, 105201.
Langer, M., Peyrin, F., 2016. 3D X-ray ultra-microscopy of bone tissue. Osteoporos. Int. 27 (2), 441–455.
Le Cann, S., Tudisco, E., Tagil, M., Hall, S.A., Isaksson, H., 2020. Bone damage evolution around integrated metal screws using X-ray tomography - in situ pullout and digital volume correlation. Front. Bioeng. Biotechnol. 8, 934.
Le Cann, S., Tudisco, E., Turunen, M.J., Patera, A., Mokso, R., Tagil, M., Belfrage, O., Hall, S.A., Isaksson, H., 2018. Investigating the mechanical characteristics of bone-metal implant interface using in situ synchrotron tomographic imaging. Front. Bioeng. Biotechnol. 6, 208.
Lin, J.D., Ozcoban, H., Greene, J.P., Jang, A.T., Djomehri, S.I., Fahey, K.P., Hunter, L.L., Schneider, G.A., Ho, S.P., 2013. Biomechanics of a bone-periodontal ligament-tooth fibrous joint. J. Biomech. 46 (3), 443–449.
Liu, L., Morgan, E.F., 2007. Accuracy and precision of digital volume correlation in quantifying displacements and strains in trabecular bone. J. Biomech. 40 (15), 3516–3520.
Lovric, G., Barre, S.F., Schittny, J.C., Roth-Kleiner, M., Stampanoni, M., Mokso, R., 2013. Dose optimization approach to fast X-ray microtomography of the lung alveoli. J. Appl. Crystallogr. 46 (Pt 4), 856–860.
Lu, X., Fernandez, M.P., Bradley, R.S., Rawson, S.D., O'Brien, M., Hornberger, B., Leibowitz, M., Tozzi, G., Withers, P.J., 2019. Anisotropic crack propagation and deformation in dentin observed by four-dimensional X-ray nano-computed tomography. Acta Biomater. 96, 400–411.
Ma, S., Goh, E.L., Jin, A., Bhattacharya, R., Boughton, O.R., Patel, B., Karunaratne, A., Vo, N.T., Atwood, R., Cobb, J.P., Hansen, U., Abel, R.L., 2017. Long-term effects of bisphosphonate therapy: perforations, microcracks and mechanical properties. Sci. Rep. 7, 43399.
Madi, K., Staines, K.A., Bay, B.K., Javaheri, B., Geng, H., Bodey, A.J., Cartmell, S., Pitsillides, A.A., Lee, P.D., 2020. In situ characterization of nanoscale strains in loaded whole joints via synchrotron X-ray tomography. Nat. Biomed. Eng. 4 (3), 343–354.
Martelli, S., Giorgi, M., Dall' Ara, E., Perilli, E., 2021. Damage tolerance and toughness of elderly human femora. Acta Biomater. 123, 167–177.
Martelli, S., Perilli, E., 2018. Time-elapsed synchrotron-light microstructural imaging of femoral neck fracture. J. Mech. Behav. Biomed. Mater. 84, 265–272.
Mastrogiacomo, M., Campi, G., Cancedda, R., Cedola, A., 2019. Synchrotron radiation techniques boost the research in bone tissue engineering. Acta Biomater. 89, 33–46.
Nagarajan, M.B., Coan, P., Huber, M.B., Diemoz, P.C., Wismuller, A., 2014. Phase contrast imaging X-ray computed tomography: quantitative characterization of human patellar cartilage matrix with topological and geometrical features. Proc. SPIE-Int. Soc. Opt. Eng. 9038, 903811.
Naghibi, H., Mazzoli, V., Gijsbertse, K., Hannink, G., Sprengers, A., Janssen, D., Van den Boogaard, T., Verdonschot, N., 2019. A noninvasive MRI based approach to estimate the mechanical properties of human knee ligaments. J. Mech. Behav. Biomed. Mater. 93, 43–51.
Naveh, G.R., Brumfeld, V., Shahar, R., Weiner, S., 2013. Tooth periodontal ligament: direct 3D microCT visualization of the collagen network and how the network changes when the tooth is loaded. J. Struct. Biol. 181 (2), 108–115.
Nazarian, A., Stauber, M., Muller, R., 2005. Design and implementation of a novel mechanical testing system for cellular solids. J. Biomed. Mater. Res. B Appl. Biomater. 73 (2), 400–411.
Obata, Y., Bale, H.A., Barnard, H.S., Parkinson, D.Y., Alliston, T., Acevedo, C., 2020. Quantitative and qualitative bone imaging: a review of synchrotron radiation microtomography analysis in bone research. J. Mech. Behav. Biomed. Mater. 110, 103887.
Oliviero, S., Giorgi, M., Dall'Ara, E., 2018. Validation of finite element models of the mouse tibia using digital volume correlation. J. Mech. Behav. Biomed. Mater. 86, 172–184.
Palanca, M., Bodey, A.J., Giorgi, M., Viceconti, M., Lacroix, D., Cristofolini, L., Dall'Ara, E., 2017. Local displacement and strain uncertainties in different bone types by digital volume correlation of synchrotron microtomograms. J. Biomech. 58, 27–36.
Pena Fernandez, M., Cipiccia, S., Dall'Ara, E., Bodey, A.J., Parwani, R., Pani, M., Blunn, G.W., Barber, A.H., Tozzi, G., 2018a. Effect of SR-microCT radiation on the mechanical integrity of trabecular bone using in situ mechanical testing and digital volume correlation. J. Mech. Behav. Biomed. Mater. 88, 109–119.
Pena Fernandez, M., Dall'Ara, E., Bodey, A.J., Parwani, R., Barber, A.H., Blunn, G.W., Tozzi, G., 2019. Full-field strain analysis of bone-biomaterial systems produced by

the implantation of osteoregenerative biomaterials in an ovine model. ACS Biomater. Sci. Eng. 5 (5), 2543–2554.
Pena Fernandez, M., Dall'Ara, E., Kao, A.P., Bodey, A.J., Karali, A., Blunn, G.W., Barber, A.H., Tozzi, G., 2018b. Preservation of bone tissue integrity with temperature control for in situ SR-MicroCT experiments. Materials 11 (11).
Pena Fernandez, M., Kao, A.P., Bonithon, R., Howells, D., Bodey, A.J., Wanelik, K., Witte, F., Johnston, R., Arora, H., Tozzi, G., 2021. Time-resolved in situ synchrotron-microCT: 4D deformation of bone and bone analogues using digital volume correlation. Acta Biomater. 131, 424–439.
Peyrin, F., Muller, C., Carillon, Y., Nuzzo, S., Bonnassie, A., Briguet, A., 2001. Synchrotron radiation microCT: a reference tool for the characterization of bone samples. Adv. Exp. Med. Biol. 496, 129–142.
Pierantoni, M., Le Cann, S., Sotiriou, V., Ahmed, S., Bodey, A.J., Jerjen, I., Nowlan, N.C., Isaksson, H., 2021a. Muscular loading affects the 3D structure of both the mineralized rudiment and growth plate at early stages of bone formation. Bone 145, 115849.
Pierantoni, M., Silva Barreto, I., Hammerman, M., Verhoeven, L., Tornquist, E., Novak, V., Mokso, R., Eliasson, P., Isaksson, H., 2021b. A quality optimization approach to image Achilles tendon microstructure by phase-contrast enhanced synchrotron micro-tomography. Sci. Rep. 11 (1), 17313.
Rapagna, S., Berahmani, S., Wyers, C.E., van den Bergh, J.P.W., Reynolds, K.J., Tozzi, G., Janssen, D., Perilli, E., 2019. Quantification of human bone microarchitecture damage in press-fit femoral knee implantation using HR-pQCT and digital volume correlation. J. Mech. Behav. Biomed. Mater. 97, 278–287.
Ridzwan, M.I.Z., Sukjamsri, C., Pal, B., van Arkel, R.J., Bell, A., Khanna, M., Baskaradas, A., Abel, R., Boughton, O., Cobb, J., Hansen, U.N., 2018. Femoral fracture type can be predicted from femoral structure: a finite element study validated by digital volume correlation experiments. J. Orthop. Res. 36 (3), 993–1001.
Roberts, B.C., Perilli, E., Reynolds, K.J., 2014. Application of the digital volume correlation technique for the measurement of displacement and strain fields in bone: a literature review. J. Biomech. 47 (5), 923–934.
Ryan, M.K., Oliviero, S., Costa, M.C., Wilkinson, J.M., Dall'Ara, E., 2020. Heterogeneous strain distribution in the subchondral bone of human osteoarthritic femoral heads, measured with digital volume correlation. Materials 13 (20).
Salome, M., Peyrin, F., Cloetens, P., Odet, C., Laval-Jeantet, A.M., Baruchel, J., Spanne, P., 1999. A synchrotron radiation microtomography system for the analysis of trabecular bone samples. Med. Phys. 26 (10), 2194–2204.
Shearer, T., Rawson, S., Castro, S.J., Balint, R., Bradley, R.S., Lowe, T., Vila-Comamala, J., Lee, P.D., Cartmell, S.H., 2014. X-ray computed tomography of the anterior cruciate ligament and patellar tendon. Muscles Ligaments Tendons J. 4 (2), 238–244.
Strotton, M.C., Bodey, A.J., Wanelik, K., Darrow, M.C., Medina, E., Hobbs, C., Rau, C., Bradbury, E.J., 2018. Optimising complementary soft tissue synchrotron X-ray microtomography for reversibly-stained central nervous system samples. Sci. Rep. 8 (1), 12017.
Tavana, S., Clark, J.N., Prior, J., Baxan, N., Masouros, S.D., Newell, N., Hansen, U., 2020a. Quantifying deformations and strains in human intervertebral discs using Digital Volume Correlation combined with MRI (DVC-MRI). J. Biomech. 102, 109604.
Tavana, S., Masouros, S.D., Baxan, N., Freedman, B.A., Hansen, U.N., Newell, N., 2020b. The effect of degeneration on internal strains and the mechanism of failure in human intervertebral discs analyzed using digital volume correlation (DVC) and ultra-high field MRI. Front. Bioeng. Biotechnol. 8, 610907.
Thurner, P.J., Wyss, P., Voide, R., Stauber, M., Stampanoni, M., Sennhauser, U., Muller, R., 2006. Time-lapsed investigation of three-dimensional failure and damage accumulation in trabecular bone using synchrotron light. Bone 39 (2), 289–299.
Titarenko, S., Titarenko, V., Kyrieleis, A., Withers, P.J., 2010. A priori information in a regularized sinogram-based method for removing ring artefacts in tomography. J. Synchrotron Radiat. 17 (4), 540–549.
Tozzi, G., Pena Fernandez, M., Davis, S., Karali, A., Kao, A.P., Blunn, G., 2020. Full-field strain uncertainties and residuals at the cartilage-bone interface in unstained tissues using propagation-based phase-contrast XCT and digital volume correlation. Materials 13 (11).
Tozzi, G., Zhang, Q.H., Tong, J., 2014. Microdamage assessment of bone-cement interfaces under monotonic and cyclic compression. J. Biomech. 47 (14), 3466–3474.
Turunen, M.J., Le Cann, S., Tudisco, E., Lovric, G., Patera, A., Hall, S.A., Isaksson, H., 2020. Sub-trabecular strain evolution in human trabecular bone. Sci. Rep. 10 (1), 13788.
Vo, N.T., Atwood, R.C., Drakopoulos, M., 2015. Radial lens distortion correction with sub-pixel accuracy for X-ray micro-tomography. Opt Express 23 (25), 32859–32868.
Vo, N.T., Atwood, R.C., Drakopoulos, M., 2018. Superior techniques for eliminating ring artifacts in X-ray micro-tomography. Opt Express 26 (22), 28396–28412.
Voide, R., Schneider, P., Stauber, M., Wyss, P., Stampanoni, M., Sennhauser, U., van Lenthe, G.H., Muller, R., 2009. Time-lapsed assessment of microcrack initiation and propagation in murine cortical bone at submicrometer resolution. Bone 45 (2), 164–173.
Wadeson, N., Basham, M., Savu, M., 2016. A Python-Based, MPI Framework for Simultaneous Processing of Multiple. N-dimensional, Large Tomography Datasets." (preprint).
Weiss, P., Obadia, L., Magne, D., Bourges, X., Rau, C., Weitkamp, T., Khairoun, I., Bouler, J.M., Chappard, D., Gauthier, O., Daculsi, G., 2003. Synchrotron X-ray microtomography (on a micron scale) provides three-dimensional imaging representation of bone ingrowth in calcium phosphate biomaterials. Biomaterials 24 (25), 4591–4601.
Yan, L., Cinar, A., Ma, S., Abel, R., Hansen, U., Marrow, T.J., 2020. A method for fracture toughness measurement in trabecular bone using computed tomography, image correlation and finite element methods. J. Mech. Behav. Biomed. Mater. 109, 103838.
Yu, B., Pacureanu, A., Olivier, C., Cloetens, P., Peyrin, F., 2020. Assessment of the human bone lacuno-canalicular network at the nanoscale and impact of spatial resolution. Sci. Rep. 10 (1), 4567.
Yue, S., Lee, P.D., Poologasundarampillai, G., Yao, Z., Rockett, P., Devlin, A.H., Mitchell, C.A., Konerding, M.A., Jones, J.R., 2010. Synchrotron X-ray microtomography for assessment of bone tissue scaffolds. J. Mater. Sci. Mater. Med. 21 (3), 847–853.
Zauel, R., Yeni, Y.N., Bay, B.K., Dong, X.N., Fyhrie, D.P., 2006. Comparison of the linear finite element prediction of deformation and strain of human cancellous bone to 3D digital volume correlation measurements. J. Biomech. Eng. 128 (1), 1–6.
Zhao, S., Arnold, M., Ma, S., Abel, R.L., Cobb, J.P., Hansen, U., Boughton, O., 2018. Standardizing compression testing for measuring the stiffness of human bone. Bone Joint Res. 7 (8), 524–538.
Zhou, Y., Hu, J., Zhou, J., Zeng, Z., Cao, Y., Wang, Z., Chen, C., Zheng, C., Chen, H., Lu, H., 2018. Three-dimensional characterization of the microstructure in rabbit patella-patellar tendon interface using propagation phase-contrast synchrotron radiation microtomography. J. Synchrotron Radiat. 25 (Pt 6), 1833–1840.
Zimmermann, E.A., Schaible, E., Bale, H., Barth, H.D., Tang, S.Y., Reichert, P., Busse, B., Alliston, T., Ager 3rd, J.W., Ritchie, R.O., 2011. Age-related changes in the plasticity and toughness of human cortical bone at multiple length scales. Proc. Natl. Acad. Sci. U. S. A. 108 (35), 14416–14421.
Zwahlen, A., Christen, D., Ruffoni, D., Schneider, P., Schmolz, W., Muller, R., 2015. Inverse finite element modeling for characterization of local elastic properties in image-guided failure assessment of human trabecular bone. J. Biomech. Eng. 137 (1).